ISSN 0010-9525, Cosmic Research, 2021, Vol. 59, No. 6, pp. 446–455. © Pleiades Publishing, Ltd., 2021.
Russian Text © The Author(s), 2021, published in Kosmicheskie Issledovaniya, 2021, Vol. 59, No. 6, pp. 473–482.

Space–Time Structure of Energetic Electron Precipitations according to the Data of Balloon Observations and Polar Satellite Measurements on February 1–6, 2015

A. D. Kugusheva[a], *, V. V. Kalegaev[a], N. A. Vlasova[a], K. A. Petrov[a], G. A. Bazilevskaya[b], and V. S. Makhmutov[b]

[a] *Skobeltsyn Institute of Nuclear Physics, Moscow State University, Moscow, 119991 Russia*
[b] *Lebedev Physical Institute, Russian Academy of Sciences, Moscow, 119991 Russia*
**e-mail: kugusheva.ad@gmail.com*

Received March 3, 2021; revised May 27, 2021; accepted June 16, 2021

Abstract—The results of an analysis of the space–time characteristics and dynamics of precipitations of magnetospheric electrons with energies in the range from 0.1 to 0.7 MeV are presented. According to the data on electron fluxes measured by vertical and horizontal detectors on the *Meteor M2*, *POES-18*, and *POES-19* satellites, particle precipitations were identified that corresponded to an event recorded during the balloon experiment carried out by the Lebedev Physical Institute on February 2, 2015. Precipitations were found at L-shells from 4 to 8 over the wide MLT range. During the event under study the regions in the near-equatorial magnetosphere have been determined, where the mechanisms are predominantly active, which are responsible for the scattering of electrons and their invasion into the Earth's atmosphere.

DOI: 10.1134/S0010952521060058

INTRODUCTION

One of the manifestations of the dynamics of the Earth's magnetosphere is the precipitation of energetic electrons from the outer radiation belt into the atmosphere. As a rule, precipitations are observed during geomagnetic disturbances, during which both the acceleration of charged particles and the scattering of captured electrons of the outer radiation belt and their precipitation into the loss cone take place [1–3]. Both of these processes may result from the development of wave activity in the magnetosphere [4, 5].

Variations in the outer electron radiation belt (RB) can occur while maintaining adiabatic invariants under the condition of relatively slow variations in the geomagnetic field in comparison with the characteristic times of electron motion. In this case, variations in electron fluxes can be recorded that are not associated with real losses or particle acceleration.

Along with the adiabatic mechanism of variations in the fluxes of trapped electrons in RBs, there are also processes that lead to real losses. A decrease in the electron flux of the outer RB can occur either due to losses at the magnetopause or during scattering into the loss cone and precipitation into the atmosphere [6, 7].

Scattering of electrons into the loss cone is associated with the violation of the adiabaticity of particle motion either in the region of a small radius of curvature of the magnetic field [8] or when interacting with low-frequency waves. Resonant interaction between electrons and VLF waves [9] and fast, time-varying, radial diffusion of electrons under the influence of ULF waves [10] are considered as the main mechanisms of electron acceleration up to relativistic energies.

Losses of particles during a geomagnetic storm occur due to pitch-angle diffusion when interacting particles with waves [11]. Variation in the pitch-angle distribution of trapped particles, leading to their precipitation into the atmosphere from the loss cone, occurs as a result of resonant interaction with low-frequency waves: magnetospheric choruses, plasmaspheric hiss, electromagnetic ion-cyclotron waves, etc. [13–15].

Precipitations of energetic electrons can be recorded directly on polar low-altitude satellites, for example, on the spacecraft of the *POES* and *Meteor* series. At the same time, balloon experiments also make it possible to detect the invasion of energetic electrons using X-ray bremsstrahlung at altitudes of 20–30 km [16, 17].

The Lebedev Physical Institute (LPI) has recorded precipitations of magnetospheric electrons ($E >$ ~100 keV) into the Earth's atmosphere from 1961 to the present in the course of a long-term balloon experiment to study the fluxes of charged particles in the Murmansk region (L = 5.5) [17]. These data are the longest homogeneous series of such measurements

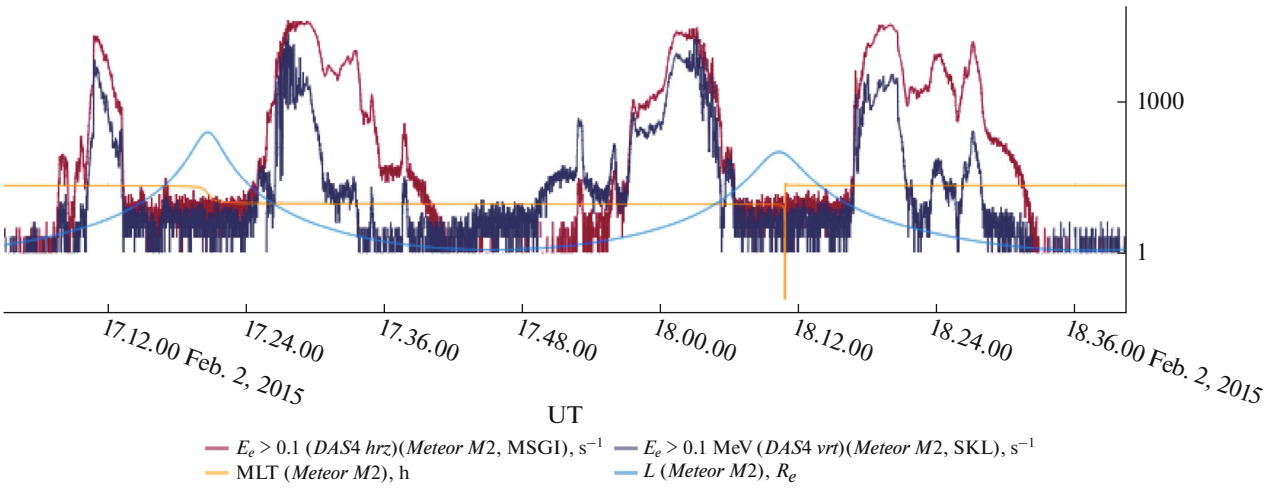

Fig. 1. Graph of electron fluxes measured by the *Meteor M2* satellite for a complete revolution.

and make it possible to study long-term variations in precipitations of energetic electrons into the atmosphere. At the same time, due to the fact that balloon experiments are usually short-lived, irregular, and attached to a longitude-limited region above the Earth's surface, they record events, whose magnetospheric sources are located in a narrow MLT sector. Thus, the magnetospheric sources of precipitations and their spatial and time characteristics remain unclear. Satellite measurements of the fluxes of precipitating energetic electrons in polar orbits make it possible to substantially enrich and supplement the data of balloon experiments. Simultaneous observations of precipitations of energetic electrons in different MLT sectors at different altitudes, their comparison with the characteristics of the interplanetary medium and geomagnetic variations make it possible to better understand the physical mechanisms of this phenomenon, as well as to establish magnetospheric sources of precipitations and their relationship with the parameters of the solar wind and the state of the magnetosphere.

In this paper, a detailed study of the event from the LPI database recorded on February 2, 2015, was carried out. Using data from measurements of electron fluxes on the *Meteor M2*, *POES-18*, and *POES-19* satellites, the spatial scales and true duration of this event were determined, and the global dynamics of precipitations of electrons with energies in the range from 0.1 to 0.7 MeV from February 1 to 6, 2015 was restored.

EXPERIMENTAL DATA

To determine the space–time characteristics of precipitations of energetic electrons, we used the data of simultaneous measurements of the polar low-orbit *Meteor M2* (Roshydromet, Russian Federation) and *POES* (NOAA, United States) spacecraft. The satellite orbits are sun-synchronous, which means that, during their entire period of operation in space, the orbital plane remains oriented in local time.

(1) Meteor M2

The Russian satellite moves in a circular sun-synchronous orbit with an altitude of 825 km and an inclination of 98.8°. The orbital period of the satellite is 101.4 min; thus, 14 revolutions around the Earth are made per day. The satellite orbit is located in the prenoon–premidnight sector of local time.

The satellite has several charged particle detectors, including a horizontal MGSI-M (DAS4, 90°) and the vertical SKL-M (DAS4, 0°). These detectors provide data on electron fluxes with energies from 100 keV to 8 MeV. At high latitudes, the vertical detector is directed approximately along the magnetic field; at near-equatorial latitudes, it is directed orthogonally to the field. With variation in latitude, the relative orientation of the detectors and the magnetic-field line varies. At high latitudes, the horizontal detector records mainly trapped particles, and the vertical one records precipitating particles.

Usually, in the region of the outer RB, an anisotropic distribution of particles is observed, when the vertical detector records the fluxes that are four to five orders of magnitude lower than the horizontal one. Scattering of particles in the magnetosphere associated with geomagnetic and wave activity leads to isotropization of particle fluxes, in this case, both detectors record close fluxes. The characteristics of the orbit make it possible to obtain data on the electron fluxes of the outer RB (at $L \sim 4$–7) four times per revolution. Figure 1 shows an example of measurements of fluxes of electrons with energies above 100 keV for a complete revolution of the satellite by vertical and horizontal detectors. Four crossings of the outer RB and flux increases can be seen according to

the vertical detector measurements, indicating electron precipitations.

(2) Polar Operational Environmental Satellites (POES)

POES is a group of polar-orbiting satellites (three of them are currently operating: *POES-15*, *POES-18*, and *POES-19*) moving in circular sun-synchronous orbits.

In this paper, we used data from two satellites: *POES-18* and *POES-19*. Their orbits are located at an altitude of 854 km above the Earth, the orbital period is 102 min, and the inclination is ~100°. The orbital plane is afternoon–after midnight (*POES-19*), and morning–evening (*POES-18*). Thus, together with *Meteor M2*, these satellites provide full and approximately uniform coverage across MLT sectors.

The satellites are equipped with the MEPED detector, which records electron fluxes in the energy range of 30 keV–2.5 MeV in the horizontal and vertical directions.

Simultaneous measurements of *Meteor M2*, *POES-18*, and *POES-19* make it possible to observe the state of the outer RB in six MLT sections in 100 min (approximately, near the directions at 2, 6, 10, 14, 18, and 22 h).

(3) ACE

The American spacecraft is located at Lagrange point *L1* between the Sun and the Earth. The complex of instruments on the spacecraft allows one to perform a wide range of observations, including the parameters of the solar wind and the interplanetary magnetic field. Simultaneous measurements of polar spacecraft and the *ACE* satellite make it possible to clarify the causal relationships between the state of the interplanetary medium and the electron fluxes of the outer ERB. At present, the *DSCOVR* spacecraft, also located in the vicinity of the *L1* point, is used to measure the parameters of the solar wind.

(4) Balloon Data

Lebedev Physical Institute records precipitations of magnetospheric electrons (E > ~100 keV) into the Earth's atmosphere from 1961 to the present in the course of a long-term experiment to study precipitations of charged particles in the upper atmosphere [17, 18]. At altitudes above 20 km, it is possible to record bremsstrahlung X-rays caused by the interaction of energetic electrons with atmospheric atoms. Below 20 km, X-rays are absorbed by the atmosphere; therefore, such observations can only be carried out at high altitudes, e.g., using balloons. The radiation intensity makes it possible to indirectly record events leading to the formation of fluxes of electrons precipitating from the magnetosphere.

Measurements in the Earth's atmosphere are carried out using standard cosmic-ray radiosonde. The detectors are a Geiger counter and a telescope of two counters. Electrons precipitating from the magnetosphere are absorbed at altitudes of more than 50 km, but they generate bremsstrahlung, which is recorded by a single counter sensitive to X-ray radiation (E > 20 keV) with an efficiency of ~1%. An increase in the counting rate of the radiosonde during electron precipitation differs from the effect of invading solar protons into the atmosphere in there being no increase in the telescope and strong variations in the particle flux. The increase in the counting rate, as a rule, begins when the probe rises to altitudes of more than 20 km. Subtracting from the data of a single counter the background formed by galactic cosmic rays, estimated from the results of previous flights of the radiosonde, it is possible to obtain the dependence of the count rate on the pressure of the residual atmosphere. Figure 2 shows examples of precipitations recorded during experiments in February, July, and November 2015.

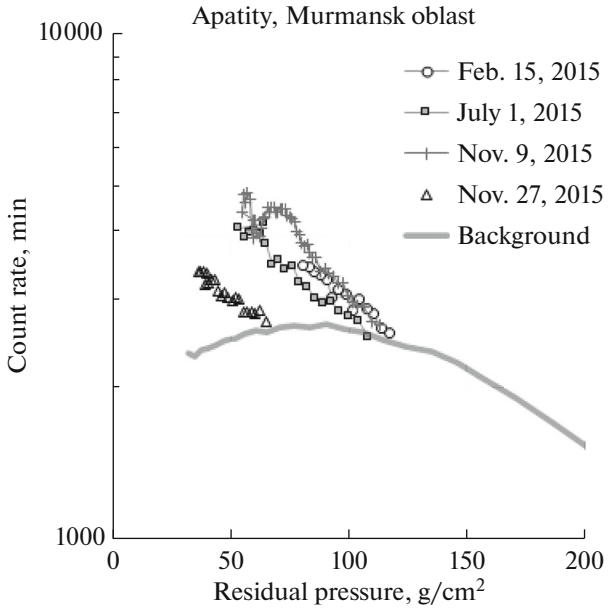

Fig. 2. Observations of balloon precipitations in the atmosphere above the Murmansk region in 2015. The background from galactic cosmic rays is shown in gray, and the increases above the background correspond to several events recorded in 2015.

In this study, we used the database created by the LPI specialists on precipitations of electrons from the Earth's outer RB [18] recorded in 2015–2017 during balloon experiments in the area of Murmansk (L = 5.5). For a detailed analysis of magnetospheric sources of precipitations, the event on February 2, 2015, was selected. The selection criteria were an intense nature of precipitation, high electron energies, and the presence of times at which the *Meteor M2* satellite at the time of precipitation recording was near the Murmansk region or at a magnetically conjugate point.

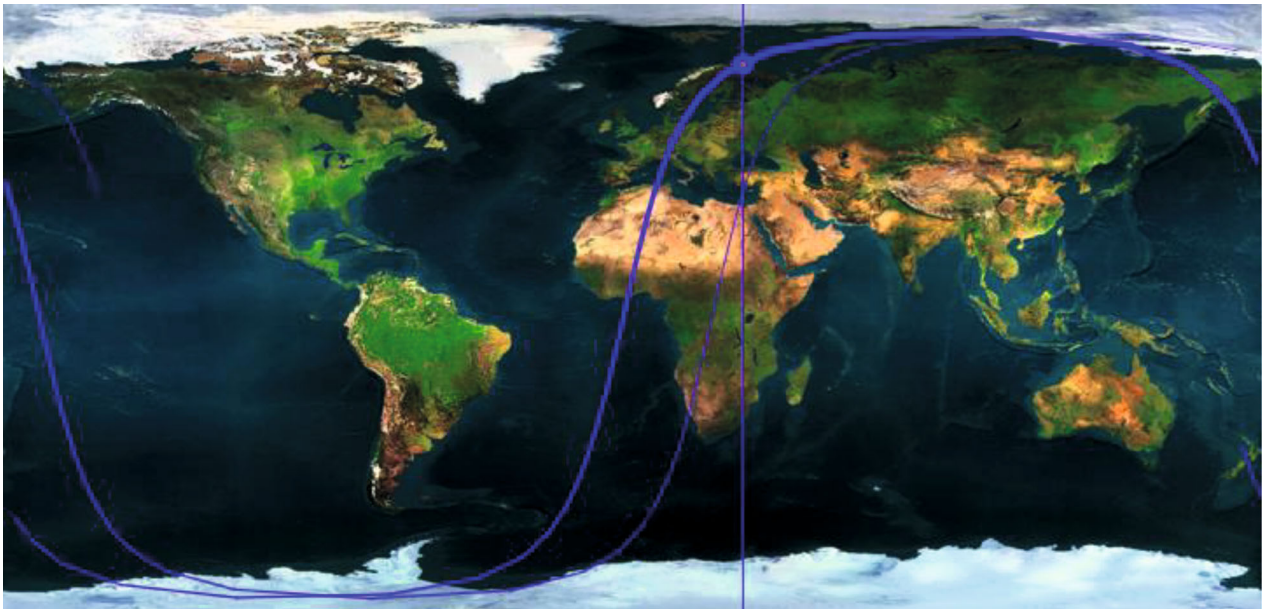

Fig. 3. Position of the *Meteor M2* satellite on February 2, 2015 at 08.56 UT.

EXPERIMENTAL RESULTS

According to the information given in the LPI database, on February 2, 2015, from 12.59 to 13.12 UT above the territory of the Murmansk region (at $L = 5.5$) during the balloon experiment, X-rays were recorded presumably associated with the scattering of trapped electrons into the loss cone and their precipitation into the atmosphere from the outer RB. The local magnetic time of the observation point on 13.00 UT was ~16 h.

By recording the increases in electron fluxes measured by the vertical detector on the *Meteor M2* satellite, particle precipitations were identified that occurred over several days and, presumably, corresponding to the event detected during balloon observations. It should be expected that the X-ray emission recorded on February 2, 2015, is a part of global event in the period from 16.38 UT on February 1, 2015, to 14.26 UT on February 6, 2015, during which precipitations were recorded by the *Meteor M2* satellite on L-shells from 4 to 7.

In the course of this event, latitudinal increases in electron fluxes with energies from 100 to 700 keV were observed, which were measured by the vertical SKL detector.

With the help of data on the satellite orbit, times closest to the event of balloon recording of X-ray radiation were found for the *Meteor M2* satellite, when it was located directly above the area of precipitation recording during the balloon experiment; in this case, electron precipitations were also observed on the satellite itself. Figure 3 shows the position of the satellite at 08.56 UT on February 2, 2015.

Figure 4 shows the time profile of fluxes of particles with 0.1 and 0.3 MeV measured by the MSGI and SKL detectors on the *Meteor M2* satellite. One can see an increase in the fluxes of precipitating electrons at the magnetic shell $L = 5.5$ at 08.56 UT on February 2, 2015, before the balloon observations. It should be noted that, due to the peculiarities of the sun-synchronous orbit of the *Meteor M2* satellite, it is, in principle, impossible for it to be above the Murmansk region at the time of the balloon launch at UT = 13 h. As already mentioned, its orbit lies in the plane of the premidnight–prenoon MLT.

For a better understanding of the causes and sources of precipitations, let us consider the conditions in the near-Earth space. It can be seen from the graphs (Fig. 5) that, in the evening of February 1, 2015, a decrease in the *Dst* index began, which reached a minimum value of –46 nT at 19.00 UT on February 2, 2015, which indicates the development of a weak geomagnetic disturbance. It can be seen that the disturbance was triggered by the variation of the IMF Bz component, which took a southerly direction on the evening of February 1, 2015.

A pressure jump is recorded in the solar wind, and the solar wind speed increases from 400 to 700 km/s, which then decreases within 3 days. These events led to the development of the storm, the recovery phase of which lasted 4 days. Fluctuations of the auroral *AE* index are also observed, which correspond to the beginning of precipitations.

According to data from low-orbit satellites, precipitations of electrons began already at the initial phase of the storm. Figure 6a shows the coordinates of the sources of precipitations of electrons with energies

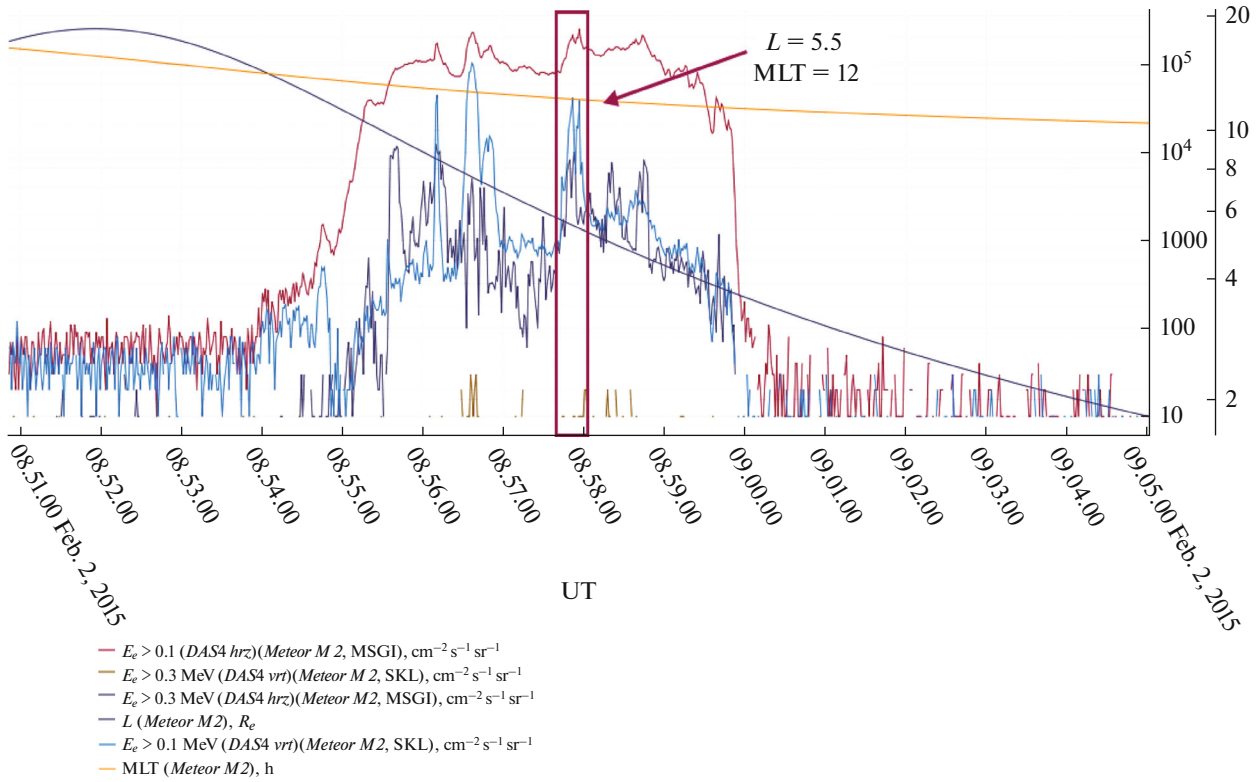

Fig. 4. Data on electron fluxes at the same time.

above 0.1 and 0.3 MeV recorded by the *Meteor M2* satellite during the initial phase of the disturbance. A polar coordinate system is used, where L acts as the radial variable and MLT as the angular variable. Each point in the graph is a projection of the coordinates of precipitations recorded in orbit by satellite measurements onto the plane of the geomagnetic equator. In fact, these are regions in the magnetosphere, where scattering of RB particles (pitch-angle diffusion) occurred, presumably associated with wave activity. When projecting onto the equatorial region, we neglect the disturbance of the geomagnetic field due to the development of magnetospheric currents, which will lead to a variation in the position of the equatorial projection of precipitations. We assume that the weak geomagnetic disturbance on February 2, 2015, did not significantly change the structure of the magnetic field lines.

The *Meteor M2* satellite allows one to measure along the meridian of ~09 and ~21 MLT. It can be seen that precipitations are mainly initiated by processes in the prenoon sector. The data obtained in the different satellite orbits indicate the probable duration of the event recorded in the course of the balloon experiment, as well as the radial dimensions, but do not allow one to judge its azimuthal extent. This requires measurement data from other satellites with trajectories located in other sectors of local time.

The *POES-18* and *POES-19* spacecraft were chosen as the sources of additional information, which provided the maximum spread in MLT values. The lower graphs in Figs. 6b and 6c show the coordinates of precipitation sources in the after-midnight and morning sectors on February 1, 2015. It can be seen that the first precipitations were recorded during 16.30–17.00 UT, when the geomagnetic disturbance began.

According to the *Meteor M2* data, the event started at 16.57 UT on February 1, 2015. The first observation of precipitations occurred in the southern hemisphere at MLT = 21.3. The fluxes of electrons with energies from 100 keV recorded by the vertical detector acquired values of 5540 $cm^{-2}\ s^{-1}\ sr^{-1}$. On the next satellite flight (17.32–17.33), precipitations of electrons with the same energies at close MLT = 20.95 are already observed above the northern hemisphere; the values of the vertical electron fluxes increased (7820 $cm^{-2}\ s^{-1}\ sr^{-1}$). Figure 7a shows the first observation of precipitations in the premidnight sector. Isotropization of 100-keV electron fluxes at L = 5.5 and 7 is visible. Precipitations have a radially localized structure.

Further flights of the satellite showed that precipitations also occurred at morning MLT values (~9). In this case, it was in the morning sector that the events had the most intense character, occurred with a higher frequency (almost continuously one after the other), and had a wide distribution region (L = 4–7), the flux values

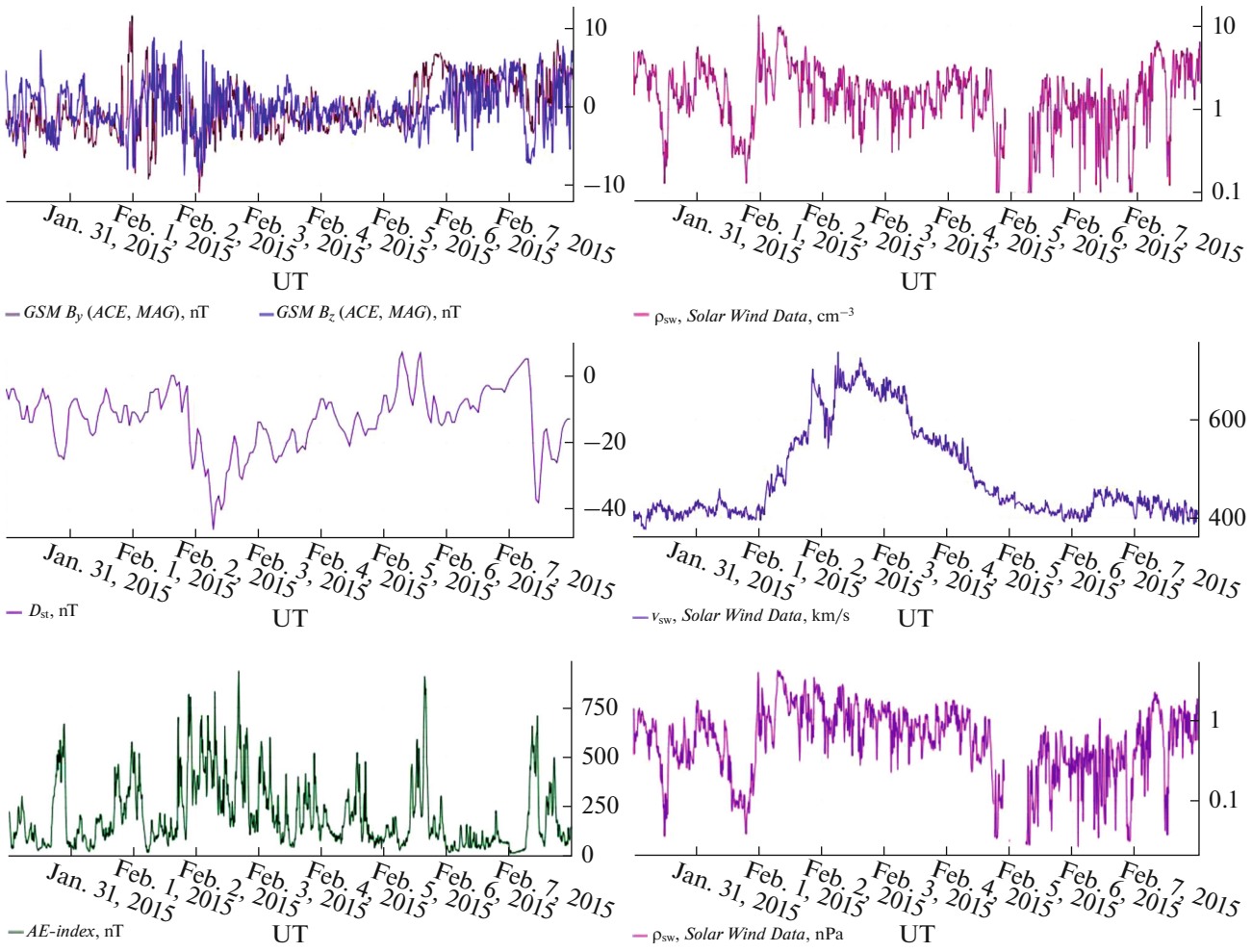

Fig. 5. Parameters of the magnetic field and solar wind in the period from January 30 to February 7, 2015.

are of the order of hundreds of thousands cm^{-2} s^{-1} sr^{-1}. At the same time, rarefied single events are observed in the evening sector, which occupy a smaller region: L = 4–6.5, the values of fluxes are of the order of tens of thousands of cm^{-2} s^{-1} sr^{-1}. This can be seen in Fig. 6a: the density of points in the morning sector is much higher. With further flights of the satellite during February 1, 2015, we see a similar picture of precipitations in both the Northern and Southern Hemisphere; in this case, the fluxes of precipitating particles increase.

The first observation of precipitations by the *POES-18* satellite took place at 17.03 UT on February 1, 2015 (Fig. 7b). The event was observed in the southern hemisphere at MLT = 4.8, L = 5–6.5. The fluxes of precipitating particles immediately assumed high values of 728854 cm^{-2} s^{-1} sr^{-1}. In the afternoon MLT sectors (~17), precipitations were initially absent. They appeared only after several spacecraft flights at 19.37 UT (Fig. 7c) and had small flux values (~3000 cm^{-2} s^{-1} sr^{-1}), which gradually increased with time, reaching values of the order of hundreds of thousands of cm^{-2} s^{-1} sr^{-1} on February 2, 2015, and later. For the morning MLT sector, precipitation profiles are observed similar to those recorded in the morning sector of the *Meteor M2* satellite.

Based on the consideration of the data on the *POES-19* satellite, a more accurate time of the beginning of the event at 16.38 UT on February 1, 2015, was established. It was first recorded in the southern hemisphere at MLT = 2.7, L = 5.6 (see Fig. 7d). As in the nighttime precipitations according to the *Meteor M2* data, the spatial localization of the precipitating electron fluxes is observed. Their values reached the value of ~250000 cm^{-2} s^{-1} sr^{-1}. On subsequent flights, precipitations were also observed in the daytime sector (MLT ~ 12), but less intense: the fluxes were the order of tens of thousands of cm^{-2} s^{-1} sr^{-1}. In the evening sector on February 1, 2015, no precipitations were observed.

The spatial structure of regions in the near-equatorial magnetosphere is shown in Fig. 8 in L-MLT coordinates and constructed according to the data from

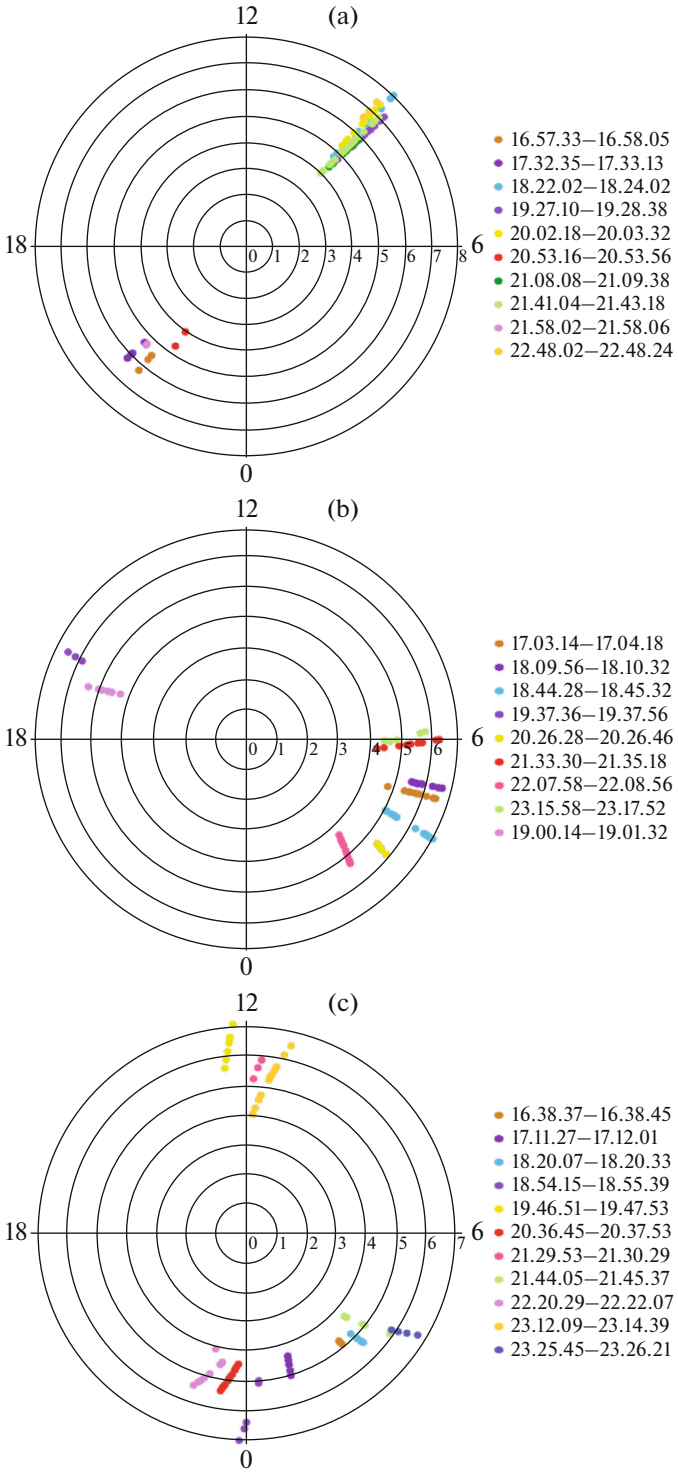

Fig. 6. Coordinates of sources of precipitations of electrons with energies in the range from 0.1 to 0.7 MeV on February 1, 2015: (a) according to the data of the *Meteor M2* spacecraft, (b) according to the data of the *POES-18* spacecraft, and (c) according to the data of the *POES-19* spacecraft.

three satellites: *Meteor M2*, *POES-18*, and *POES-19*. These regions are sources of energetic electron precipitations during the disturbed period on February 1–6, 2015. It can be seen (Fig. 8a) that, by the evening of February 1, 2015, in the initial period of disturbances, the region of precipitations covered mainly the morning, night, and, partly, the day sector. Also, the first precipitations appeared on the afternoon MLT.

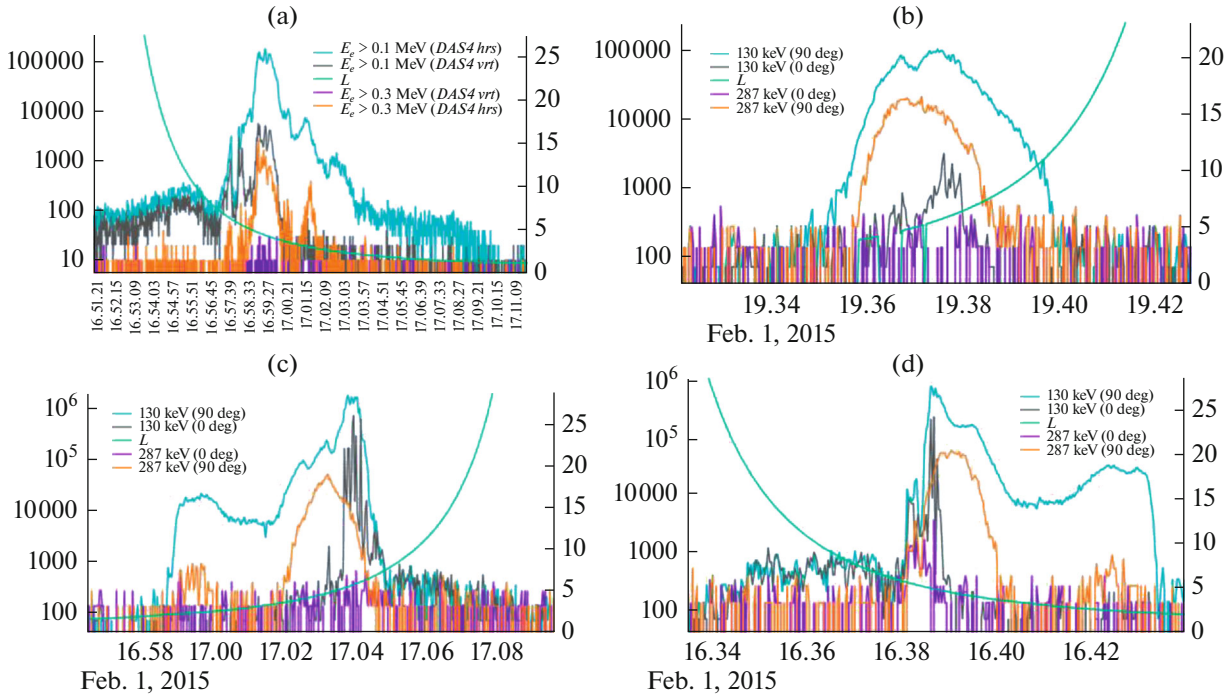

Fig. 7. Electron fluxes: (a) *Meteor M2* first observation of precipitations (premidnight sector), (b) *POES-18*, first observation of precipitations; (c) *POES-18* initiation of precipitations in the evening sector, and (d) *POES-19*, first observation of precipitations.

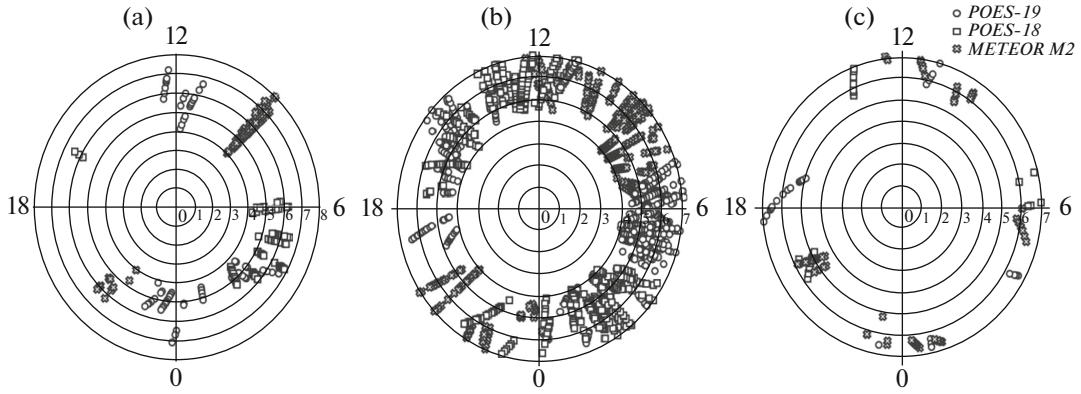

Fig. 8. Coordinates of precipitation sources according to the data of three satellites: (a) February 1, 2015, is the beginning of the event; (b) February 2, 2015; and (c) February 6, 2015 is the end of the event.

Figure 8b shows a map of precipitations at the main phase of geomagnetic disturbance. It can be seen that precipitations have trapped almost all sectors of the magnetosphere and are recorded in a wide range of L (from 4 to 7) and at all longitudes.

The event ended in the morning of February 6, 2015. By this time, the fluxes of precipitating electrons became more localized along L, and the fluxes decreased and reached values of the order of 10000 $cm^{-2}\,s^{-1}\,sr^{-1}$ at the end of the event. The graph (Fig. 8c) shows the distribution of precipitation sources according to the data of three satellites over MLT and L for the period from 00.00 to 14.26 UT on February 6, 2015. It can be seen from this graph that the occupied area of precipitations covers all MLTs, but there were significantly fewer events, which were located at more distant MLT > 5 and more isolated.

RESULTS AND DISCUSSION

According to the data on the parameters of the solar wind and the interplanetary magnetic field, it was found that precipitations of electrons with energies in the range from 0.1 to 0.7 MeV and higher

occurred in the geomagnetically disturbed magnetosphere. Observations of satellites made it possible to approximately determine the beginning of the event (16.38 UT on February 1, 2015) and the space–time characteristics of the precipitation region during the entire period of magnetospheric disturbances.

Summarizing the observational data of three polar satellites, we can conclude that, at the initial stage of disturbances, precipitations developed at $L > 5$ in the MLT night sector and had an isolated character. The electron fluxes were hundreds of thousands of $cm^{-2}\ s^{-1}\ sr^{-1}$. Gradually, precipitations moved to the morning region of the magnetosphere and, at the main phase of geomagnetic disturbance, filled the entire 0–12 MLT sector. The precipitation profiles differed from those in the nighttime magnetosphere. They had the form of multiple bursts in the relatively wide interval of L from 4 to 7.

At the main phase and the initial stage of the recovery phase (February 2, 2015), precipitations occupied both the daytime and evening sectors, thus covering all THE MLT values, but, in the evening sector, precipitations had a quieter character and the particle fluxes were about 10000 $cm^{-2}\ s^{-1}\ sr^{-1}$. It can be claimed that X-ray bremsstrahlung associated precisely with these electron fluxes was observed during the balloon experiment on February 2, 2015.

Based on the position and nature of precipitations, it can be assumed that the mechanisms of acceleration and scattering of particles were of a different nature in different regions of the magnetosphere. Precipitations in the nighttime magnetosphere had an isolated, radially localized character at relatively high latitudes ($L > 5$). Apparently, these events are associated with the scattering of electrons in the strongly curved magnetic field of the geomagnetic tail and can be attributed to the Group 1 precipitations according to the classification in [8]. The generation of such precipitations is associated with the approach of the magnetosphere tail current sheet during a geomagnetic disturbance. Precipitations in the sector with MLT in the range from 0 to 12 are associated with the generation of VLF waves—auroral chorus and whistlers, which cause both the acceleration of electrons and their scattering into the loss cone [19].

A drop in the *Dst* index to –46 nT and the negative value of the *Bz* component of the magnetic field indicate the development of a moderate geomagnetic storm, during the recovery phase of which the main precipitations of electrons were observed. Variations in the *AE* index at the time when the IMF *Bz* component took a southerly direction, as well as the *AE* index values of the order of hundreds of nT during the beginning and recovery phase of the storm, indicate a sequence of substorms that caused the scattering of high-energy electrons into the loss cone and further precipitations into the atmosphere in the sector from 0 to 12 MLT, which is an important factor for the appearance of a VLF chorus and other low-frequency waves in the auroral magnetosphere [20]. Substorms also led to the generation of electromagnetic equatorial noise and VLF hiss in the afternoon sector, which were responsible for precipitations on daytime and evening MLTs. The precipitations had a wide MLT length and a maximum probability of observation at night and in the morning. According to the classification of electron precipitations in [8, 21], nighttime precipitations belongs to the first type. Precipitations in the morning sector are apparently associated with multiple substorm activations at the main phase of the storm and the subsequent scattering of particles into the loss cone [20].

CONCLUSIONS

Using data from satellites of the *POES* and *Meteor* series, a space–time analysis was carried out and the dynamics of the event on February 1–6, 2015, of precipitations of electrons with energies in the range from 0.1 to 0.7 MeV into the Earth's atmosphere, corresponding to the event on February 2, 2015, from the LPI database, was considered. A connection was established between the data on particle fluxes and data on the magnetic field and solar wind, which made it possible to make a hypothesis about the mechanisms of precipitation occurrence and explain their observed dynamics, as well as classify this event.

ACKNOWLEDGMENTS

This study was supported by the Russian Foundation for Basic Research, project no. 19-05-00960.

REFERENCES

1. Thorne, R.M., Radiation belt dynamics: The importance of wave-particle interactions, *Geophys. Rev. Lett.,* 2010, vol. 37, no. 22.
2. Baker, D.N., Erickson, P.J., Fennell, J.F., et al., Space weather effects in the Earth's radiation belts, *Space Sci. Rev.,* 2018, vol. 214, id. 17. https://doi.org/10.1007/s11214-017-0452-7
3. Wu, H., Chen, T., Kalegaev, V.V., Panasyuk, M.I., Vlasova, N.A., and Duan, S., Long-term dropout of relativistic electrons in the outer radiation belt during two sequential geomagnetic storms, *J. Geophys. Res. Space Phys.,* 2020, vol. 125, no. 10, id. e2020JA028098.
4. Horne, R.B. and Thorne, R.M., Potential waves for relativistic electron scattering and stochastic acceleration during magnetic storms, *Geophys. Rev. Lett.,* 1998, vol. 25, no. 15, pp. 3011–3014.
5. Lazutin, L.L., Dmitriev, A.V., and Suvorova, A.V., Electron radiation belt dynamics during magnetic storms and in quiet time, *Sol.-Terr. Phys.,* 2018, vol. 4, no. 1, pp. 59–71.
6. Shprits, Y.Y., Thorne, R.M., Friedel, R., et al., Outward radial diffusion driven by losses at magnetopause,

J. Geophys. Res., 2006, vol. 111, id. A11214. https://doi.org/10.1029/2006JA011657

7. Blum, L.W. and Breneman, A.W., Observations of radiation belt losses due to cyclotron wave-particle interactions, *Loss in the Magnetosphere to Particle Precipitation in the Atmosphere,* Amsterdam: Elsevier, 2020, pp. 49–98.
8. Yahnin, A.G., Yahnina, T.A., Semenova, N.V., et al., Relativistic electron precipitation as seen by NOAA *POES, J. Geophys. Res. Space Phys.,* 2016, vol. 121, pp. 8286–8289. https://doi.org/10.1002/2016JA022765
9. Horne, R.B., Thorne, R.M., Glauert, S.A., et al., Timescale for radiation belt electron acceleration by whistler mode chorus waves, *J. Geophys. Res.,* 2005, vol. 110, id. A03225. https://doi.org/10.1029/2004HA010811
10. Ukhorskiy, A.Y., Anderson, B.J., Brandt, P.C., and Tsyganenko, N.A., Storm time evolution of the outer radiation belt: transport and losses, *J. Geophys. Res. Space Phys.,* 2006, vol. 111, id. A11S03. https://doi.org/10.1029/2006JA011690
11. Tverskoi, B.A., *Dinamika radiatsionnykh poyasov Zemli* (Dynamics of the Earth's Radiation Belts), Moscow: Nauka, 1968.
12. Meredith, N.P., Horne, R.B., Lam, M.M., et al., Energetic electron precipitation during high-speed solar wind stream driven storms, *J. Geophys. Res.,* 2011, vol. 116, id. A05223. https://doi.org/10.1029/2010JA016293
13. Shprits, Y.Y., Subbotin, D.A., Meredith, N.P., and Elkington, S., Review of modeling of losses and sources of relativistic electrons in the outer radiation belt II: local acceleration and losses, *J. Atm. Sol.-Terr. Phys.,* 2008, vol. 70, pp. 1694–1713. https://doi.org/10.1016/j.jastp.2008.06.014
14. Xiao, F., Chang Yang, Zhaoguo He, et al., Chorus acceleration of radiation belt relativistic electrons during March 2013 geomagnetic storm, *J. Geophys. Res. Space Phys.,* 2014, vol. 119, pp. 3325–3332. https://doi.org/10.1002/2014JA019822
15. Lazutin, L.L., *Rentgenovskoe izluchenie avroral'nykh elektronov i dinamika magnitosfery* (X-Ray Emission of Auroral Electrons and Dynamics of the Magnetosphere), Leningrad: Nauka, 1979.
16. Makhmutov, V.S., Bazilevskaya, G.A., Stozhkov, Yu.I., et al., Catalogue of electron precipitation events as observed in the long-duration cosmic ray balloon experiment, *J. Atm. Sol.-Terr. Phys.,* 2016, vol. 149, pp. 258–276.
17. Bazilevskaya, G.A., Kalinin, M.S., Krainev, M.B., et al., Precipitation of magnetospheric electrons into the Earth's atmosphere and electrons of the outer radiation belt, *Izv. Ross. Akad. Nauk. Ser. Fiz.,* 2017, vol. 81, no. 2, pp. 235–238.
18. Omura, Y., Nunn, D., and Summers, D., Generation processes of whistler-mode chorus emissions: Current status of nonlinear wave growth theory, *Dynamics of the Earth's Radiation Belts and Inner Magnetosphere,* Washington, DC: American Geophysical Union, 2012.
19. Tsurutani, B.T., et al., Are high-intensity long-duration continuous AE activity (HILDCAA) events substorm expansion events?, *J. Atm. Sol.-Terr. Phys.,* 2004, vol. 66, no. 2, pp. 167–176.
20. Yakhnina, T.A., Yakhnin, A.G., and Semenova, N.V., Relationship between relativistic electron precipitation and geomagnetic activity, *Physics of Auroral Phenomena, Proc. XXXVIII Annual Seminar, Apatity,* 2015, pp. 75–78.

Translated by N. Topchiev